Bubble Growth by Coalescence in Gas Fluidized Beds

DIMITRIS T. ARGYRIOU, HARVEY L. LIST, and REUEL SHINNAR

The City College, CUNY, New York, New York

Bubble size and distribution of bubble sizes were studied in an air fluidized bed, 11.5 in. in diam. and 3 ft. high, by taking motion pictures of the bubbles breaking the top surface of the bed and by determining the size of the bubbles from the film. The distribution of bubble volumes at a given bed height was expressed as a gamma distribution with parameters obtained from the observations. A statistical mechanical method proposed by Hulburt and Katz for studies in agglomeration of particles was used in the mathematical formulation of the problem. A proposed mechanism of bubble growth by coalescence in gas fluidized beds resulted in a one parameter model. Comparisons of the distributions predicted by the model to the experimentally obtained profiles yielded the parameter of the model.

In gas fluidized beds the gas in excess of that required for incipient fluidization passes through the bed as bubbles. These bubbles grow as they travel up the bed, mainly because of collisions with other bubbles. Average size and size distribution of bubbles are needed in the design of fluidized beds in gas-solids contact for mass transfer, heat transfer, and chemical reactions where, for example, a gaseous reaction is catalyzed by the fluidized solids (*2, 3*).

Bubble growth has been investigated by various researchers. Experimenting with transparent wall beds, Ohmae and Furukawa (*4*) and Mathis and Watson (*5*) observed that bubbles adjacent to the wall increase in size, owing to coalescence. Morse and Ballou (*6*), Yasui and Johanson (*7*), Lanneau (*8*), and Porter (*9*) studied bubble characteristics by means of probes submerged into the bed. Grohse (*10*) and Baumgarten and Pigford (*11*) used radiation absorption techniques to measure density fluctuations in the path of a beam through fluidized beds. Romero and Smith (*12*) used a flash x-ray method to study internal structure of 3-in.-square fluidized beds. They obtained instantaneous pictures of an 11-in.-high part of the bed.

Results obtained by these methods are somewhat difficult to interpret. Use of the submerged probe, for example, may disturb the bubbles; also there is no way of knowing whether passage of a bubble through the probes is symmetrical when a diameter is recorded or off-center when a chord is recorded. Although the radiation absorption and flash x-ray techniques do not disturb the bubbles, these methods can not distinguish one bubble behind the other in the path of the rays. Useful results, however, were obtained about bubbling fluidized beds as follows:

1. Bubbles grow in size as they travel up the bed while bubbling frequency decreases.
2. At a given bed height, bubbles are larger at higher flow rates.
3. Larger bubbles travel up the bed faster than smaller ones.

Harrison and Leung (*13*) investigated the coalescence of bubbles injected one behind the other into an incipiently fluidized bed. They found that the time required for the second bubble to catch up with the first increases by increasing the initial distance between the two bubbles. They also found that with the same separation, the catch-up time is smaller for larger bubbles.

In the present work bubble sizes in gas fluidized beds were quantitatively determined. By taking movies of the top surface of the bed, the number of bubbles per unit bed height, average bubble volume, and variance of bubble volumes were obtained as a function of bed height. Results were compared to the values predicted by a model based on a proposed mechanism of bubble coalescence yielding the parameter of the model.

MATHEMATICAL MODEL

The mathematical development follows that of Hulburt and Katz (*1*). Two sets of coordinates describe the bubble, an external one specifying its location (that is, the vertical distance z from the origin) and an internal one specifying its dimensions (that is, the bubble volume m). The number density of the bubbles $f(z, m, t)$ is defined so that $f(z, m, t)\ dzdm$ is the number of bubbles at time t in a slice of bed from $z - dz/2$ to $z + dz/2$ and having volumes from $m - dm/2$ to $m + dm/2$. A function $h(z, m, t)$ representing the net rate of introduction of bubbles into the system is also defined so that $h(z, m, t)\ dzdm$ is the net number of bubbles having volumes from $m - dm/2$ to $m + dm/2$ introduced per unit time, at time t, into a slice of bed from $z - dz/2$ to $z + dz/2$ by means other than flow.

The conservation of bubble volume yields

$$\frac{\partial f}{\partial t} + \frac{\partial (vf)}{\partial z} = h \qquad (1)$$

Collisions between bubbles of volumes m_1 and m_2 are

Dr. Argyriou is with E. I. du Pont de Nemours & Co., Wilmington, Delaware.

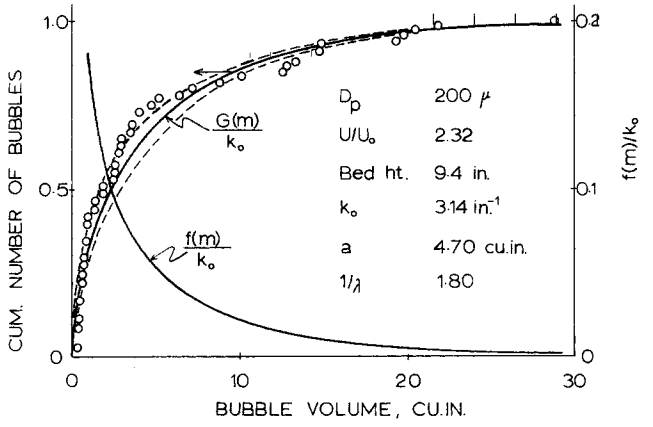

Fig. 1. Distribution of bubble volumes (0 to 30 cu. in.).

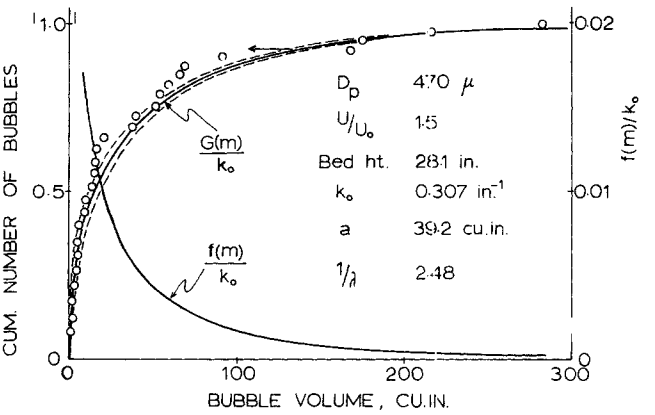

Fig. 2. Distribution of bubble volumes (0 to 300 cu. in.)

assumed to be proportional to the product of the number densities of the two species and the mean projected area of the two bubbles. The rate of formation of bubbles of volume m by coalescence then is

$$r_f = \frac{B}{2S} \int f(z, m', t)$$

$$f(z, m - m', t)\ [m'^{1/3} + (m - m')^{1/3}]^2\, dm' \quad (2)$$

and the rate of loss of bubbles of volume m because of collisions with other bubbles is

$$r_e = \frac{B}{S} f(z, m, t) \int f(z, m', t)\ (m^{1/3} + m'^{1/3})^2\, dm' \quad (3)$$

where S is the cross sectional area of the bed. The integration is taken over all possible values of m' in each case.

B is a collision parameter with dimensions of velocity. It is proportional to the relative velocity of the colliding bubbles and results by multiplying this relative velocity by the collision efficiency (fraction of collisions resulting in coalescence) and the numerical factor $\frac{\pi}{4}\left(\frac{6}{\pi}\right)^{2/3}$ resulting from the expressions $(m_1^{1/3} + m_2^{1/3})^2$. B might really be a function of m and $(m - m')$, but as a first approximation we assume it to be a constant. This assumption has led to reasonable results in the study of other coalescence phenomena.

Combining these two rates gives

$$h(z, m, t) = \frac{B}{S}\left\{\frac{1}{2}\int f(z, m', t)\, f(z, m - m', t)\right.$$
$$[m'^{1/3} + (m - m')^{1/3}]^2\, dm' - f(z, m, t)$$
$$\left.\int f(z, m', t)\,(m^{1/3} + m'^{1/3})^2\, dm'\right\} \quad (4)$$

Substituting Equation (4) into (1) yields

$$\frac{\partial f}{\partial t} + \frac{\partial (vf)}{\partial z} = \frac{B}{S}\left\{\frac{1}{2}\int f(z, m', t)\right.$$
$$f(z, m - m', t)\ [m'^{1/3} + (m - m')^{1/3}]^2\, dm'$$
$$\left. - f(z, m, t) \int f(z, m', t)\,(m^{1/3} + m'^{1/3})^2\, dm'\right\} \quad (5)$$

The velocity may be expressed as a function of bubble volume m (9, 12, 14, 15, 16)

$$v = Am^{1/6} \quad (6)$$

where A is a constant.

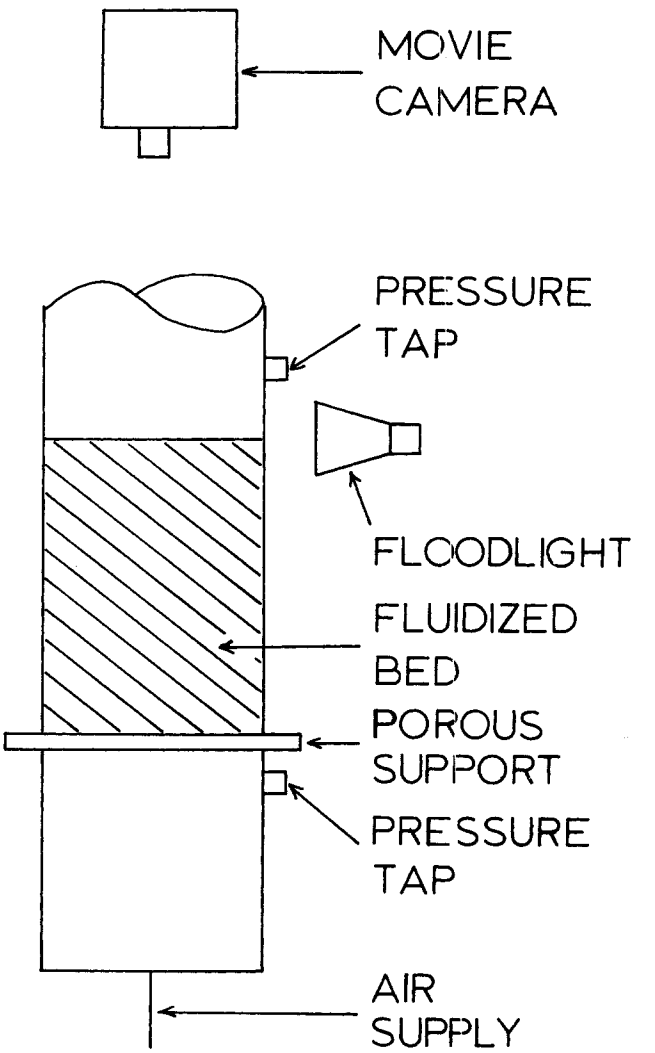

Fig. 3. Diagram of fluidization unit showing position of flood-lamp and movie camera.

Substituting this in Equation (5) and considering steady state we obtain

$$\frac{m^{1/6} df(z, m)}{dz} = b\left\{\frac{1}{2}\int f(z, m') f(z, m - m')\right.$$
$$[m'^{1/3} + (m - m')^{1/3}]^2\, dm'$$
$$\left. - f(z, m) \int f(z, m')\,(m^{1/3} + m'^{1/3})^2\, dm'\right\} \quad (7)$$

where $b = B/AS$ is a new constant.

Fig. 4. Top bed surface (2.4 in. high).

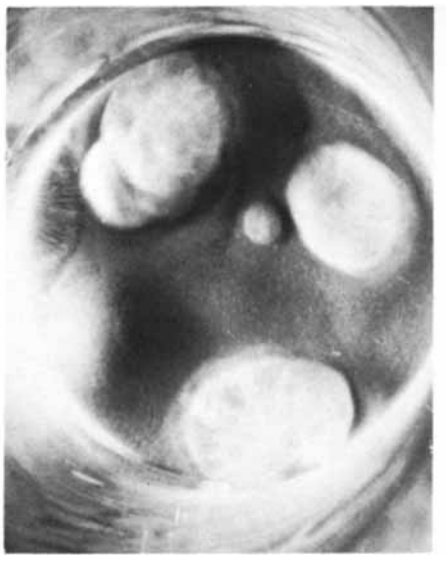

Fig. 5. Top bed surface (9.1 in. high).

Fig. 6. Top bed surface (26.7 in. high).

Equation (7) describes the steady state evolution of the number density with bed height. It may be simplified by applying moment methods on it, thus yielding a set of differential equations for the moments of m. These moments are defined as

$$\mu_j = \int_0^\infty m^j f(z, m)\, dm; \quad j \geqq 0 \tag{8}$$

(μ_0 is therefore the total number of bubbles per unit bed height, μ_1 their total volume, etc.)

Using moments on Equation (7) gives

$$\frac{d\mu_{n+1/6}}{dx} = \frac{1}{2}\sum_{r=0}^{n}\binom{n}{r}(\mu_{n-r+2/3}\mu_r + 2\mu_{n-r+1/3}\mu_{r+1/3} + \mu_{n-r}\mu_{r+2/3}) - (\mu_0\mu_{n+2/3} + 2\mu_{1/3}\mu_{n+1/3} + \mu_{2/3}\mu_n)$$

$$n = 0, 1, 2, \ldots; \quad \binom{n}{r} = \frac{n!}{(n-r)!r!} \tag{9}$$

Here the transformation $x = bz$ was used.

The first three equations obtained from (9) for $n = 0$, 1, and 2, respectively, are:

$$\frac{d\mu_{1/6}}{dx} = -(\mu_0\mu_{2/3} + \mu_{1/3}^2) \tag{10}$$

$$\frac{d\mu_{7/6}}{dx} = 0 \tag{11}$$

$$\frac{d\mu_{13/6}}{dx} = 2(\mu_1\mu_{5/3} + \mu_{4/3}^2) \tag{12}$$

These equations contain too many unknowns and they do not close for any n. Approximate solutions, however, may be sought by expanding $f(x, m)$ into a Laguerre series:

$$f(m) = \frac{\lambda}{a}p^{(\lambda)}\left(\frac{\lambda m}{a}\right)\sum_{i=0}^{\infty} k_i L_i^{(\lambda)}\left(\frac{\lambda m}{a}\right) \tag{13}$$

where

$$p^{(\lambda)}(z) = \frac{1}{(\lambda-1)!}z^{\lambda-1}e^{-z} \tag{14}$$

is the Γ distribution and

$$L_i^{(\lambda)}(z) = \sum_{j=0}^{i}(-1)^j\frac{i!\,(i+\lambda-1)!}{j!\,(i-j)!\,(i+\lambda-1-j)!}z^{i-j}; \quad i = 0, 1, 2, \ldots \tag{15}$$

are the associated Laguerre polynomials.

This series is developed so that the first term contains three parameters, k_0, a, and λ, and the second and third terms drop out. As $f(m)$ is a function of x, the parameters k_0, a, and λ are expected to be functions of x also. The three parameters are

$$k_0 = \mu_0 \tag{16}$$

$$a = \mu_1/\mu_0 \tag{17}$$

$$\lambda = \frac{a^2}{\mu_2/\mu_0 - a^2} \tag{18}$$

Hence k_0 is the total number of bubbles per unit bed height, a is the mean bubble volume, and a^2/λ the variance of bubble volumes. Here only the first term of the series was used, i.e., the distribution of bubble volumes

Table 1. Properties of Glass Beads

Density: 156 lbs./cu.ft.

Average diameter, μ		Size distribution				Bulk density, lb./cu.ft.
470	U. S. Sieve No.	20	40	50	60	93.7
	% retained	0	70	25	5	
200	U. S. Sieve No.	60	70	80	100	94.2
	% retained	10	40	40	10	
85	U. S. Sieve No.	170	200	230	270	93.6
	% retained	15	65	15	5	

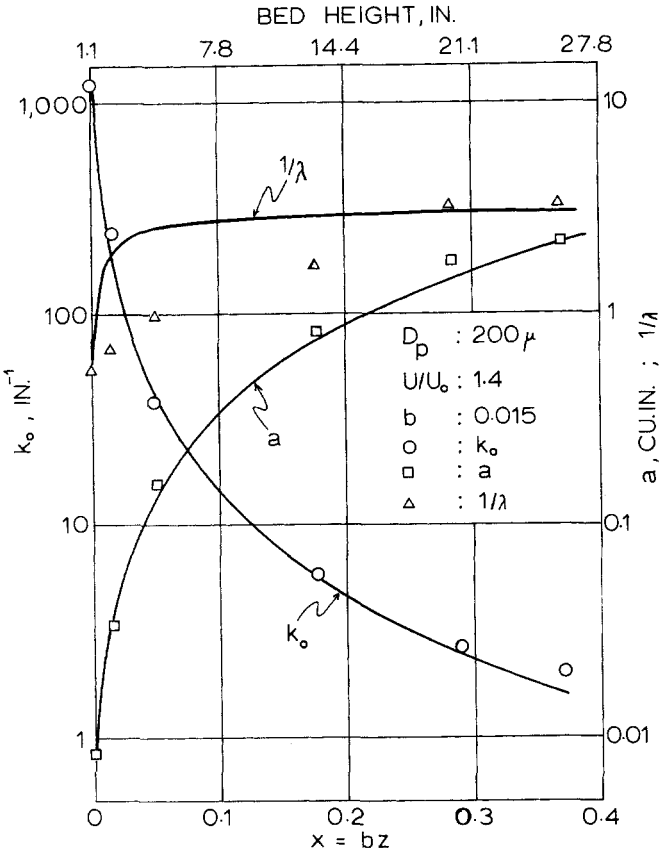

Fig. 7. Experimental and predicted values of k_0, a, $1/\lambda$ in beds of glass beads.

was represented by a Γ distribution.

$$f(m) = \frac{\lambda k_0}{a} \cdot \frac{1}{(\lambda - 1)!} \left(\frac{\lambda m}{a}\right)^{\lambda - 1} e^{-\frac{\lambda m}{a}} \qquad (19)$$

This distribution is shown in Figures 1 and 2 where the circles represent experimental values of the normalized cumulative number of bubbles plotted against bubble volume. The solid line is the normalized incomplete Γ function

$$\frac{G(m)}{k_0} = \int_0^m \frac{f(m')}{k_0}\, dm'$$

$$= \int_0^m \frac{\lambda}{a} \cdot \frac{1}{(\lambda - 1)!} \left(\frac{\lambda m'}{a}\right)^{\lambda - 1} e^{-\frac{\lambda m'}{a}}\, dm' \qquad (20)$$

with parameters k_0, a, and λ calculated from the data. The normalized Γ distribution $f(m)/k_0$ also is shown in the figures. Using moments (19) yields

$$\mu_n = k_0 \left(\frac{a}{\lambda}\right)^n \frac{(n + \lambda - 1)!}{(\lambda - 1)!}; \quad n \geqq 0 \qquad (21)$$

With the aid of Equation (21), moments are expressed in terms of the three parameters of the distribution k_0, a, λ. Equations (10) to (12) are transformed now into a set of equations in k_0, a, λ:

$$\frac{dk_0}{dx} = \frac{-k_0^2 a^{1/2}}{36} \left\{ 42R(\lambda) - \lambda Q(\lambda) \left[P(\lambda) - \frac{\lambda}{1 + 6\lambda} \right] \right\} \qquad (22)$$

$$\frac{da}{dx} = \frac{k_0 a^{3/2}}{36} \left[36R(\lambda) - \frac{\lambda}{1 + 6\lambda} Q(\lambda) \right] \qquad (23)$$

$$\frac{d(1/\lambda)}{dx} = \frac{k_0 a^{1/2}}{36} Q(\lambda) \qquad (24)$$

where

$$R(\lambda) = \frac{1}{\sqrt{\lambda}} \left[\frac{\Gamma\left(\lambda + \frac{2}{3}\right)}{\Gamma\left(\lambda + \frac{1}{6}\right)} + \frac{\Gamma^2\left(\lambda + \frac{1}{3}\right)}{\Gamma(\lambda)\Gamma\left(\lambda + \frac{1}{6}\right)} \right] \qquad (25)$$

$$P(\lambda) = \lambda \left[\psi\left(\lambda + \frac{1}{6}\right) - \psi(\lambda) \right] \qquad (26)$$

$$Q(\lambda) = \frac{1}{\lambda^{5/2}} \left[\frac{\Gamma^2\left(\lambda + \frac{1}{3}\right)}{\Gamma(\lambda)\Gamma\left(\lambda + \frac{1}{6}\right)} - 7\frac{\Gamma\left(\lambda + \frac{2}{3}\right)}{\Gamma\left(\lambda + \frac{1}{6}\right)} \right] + 36R(\lambda) \qquad (27)$$

Here $\Gamma(a) = (a - 1)!$ is the gamma function and $\psi(a) = \frac{d \ln \Gamma(a)}{da}$ is the digamma function, both tabulated (*17*). Relations (22) to (24) constitute a set of coupled ordinary differential equations that, with proper initial conditions, can be solved to yield the profiles k_0, a, λ as they develop in x.

Initial Conditions

Bubble formation in gas fluidized beds is not yet well understood. Jackson (*18*), Pigford and Baron (*19*), and Porter (*9*) consider bubbles as the outgrowth of small local disturbances in the distribution of particles and voids of a uniformly fluidized bed. Employing a linearized stability analysis, they found that small local disturbances in the number of particles per unit bed volume propagate both upward and downward in the bed from their point of origin. The downward components are damped out rapidly while the upward components increase in amplitude exponentially as they propagate, giving rise to instability. These theories, however, apply only to infinitesimal disturbances and may describe the initial rate of growth of small disturbances. Once the disturbances have grown to finite size, the nonlinearities of the original equations, which were ignored in the analysis, may become important; conclusions may not be drawn on finite size disturbances or "bubbles." Davidson and Harrison (*20*) suggest that voids of a size equal to that of the particles characterize a bed at incipient fluidization. Voids ten times the particle size are considered bubbles. Voids of sizes between 1 and 10 define a transition from particulate to aggregative fluidization. Even this simple demarcation does not give a complete set of initial conditions to be used with Equations (22) to (24). Because initial conditions can not at present be derived on first principles, the equations were solved with initial conditions, the experimentally obtained distribution at the lowest bed height.

TABLE 2. PROPERTIES OF CRACKING CATALYST

Bulk density: 32.5 lbs./cu.ft. (loosely packed)
Density: 153 lbs./cu.ft.
Particle density: 55 lbs./cu.ft.

Size distribution (micromesh analysis)

Size, μ	0-20	0-40	0-80	0-105	0-149
Weight, %	2	21	77	92	99

EQUIPMENT AND EXPERIMENTS

Equipment

The fluidization unit consisted of a clear wall plastic column 11.5 in. I.D., flanged into a porous stainless steel support plate (see Figure 3). The surface of the bed was illuminated by floodlights. Two movie cameras*—an 18-mm. and a 35-mm., both with adjustable speeds—were used.

Procedure

At any particular run the height of the bed at rest was measured, and the bed was fluidized at a high air flow rate. The flow was maintained at this level for several minutes and then reduced to the desired level. Air flow rate, temperature, and pressure were recorded along with pressure drop across the bed. The floodlights were turned on, the camera was adjusted for the right distance and lens opening, and the motion pictures were taken for a prescribed time interval. Air flow conditions and pressure drop along the bed were again checked and the run was completed.

The frames of the developed film were numbered consecutively starting with 1 for each run, and these numbers served as the time calibration of the runs. The numbered film was projected on coordinate paper and frame number, coordinates of the center, and diameter were recorded for each bubble just before bursting. For bubbles that were not round, the geometric mean of the maximum d_{max} and minimum d_{min} measured dimensions were recorded as the diameter d_i

$$d_i = \sqrt{d_{max}\, d_{min}} \qquad (28)$$

The inside diameter of the tube was used as a reference for calibrating lengths. Incipient fluidizing velocity for each solid was taken as the maximum velocity at which no bubbles appear in a 4 in. high bed.

Materials

Glass beads (Table 1) of narrow size distribution and cracking catalyst† (Table 2) of wide size distribution were fluidized with air. When the catalyst was fluidized, its very fine particles formed a cloud of dust which filled the containing column above the bed surface and created poor visibility for taking motion pictures.

These unsuitable conditions were overcome by fluidizing the catalyst for 1 hr. at 0.54 ft./sec. air velocity and allowing the dust to be carried away. Because the catalyst then lost 5% of its original volume, its size distribution in the experiments was somewhat different from the one given in Table 2, with most of the 0 to 20μ and some of the 20 to 40μ fractions missing. No size distribution determination of the treated material was made.

INTERPRETATION OF DATA

From data available by direct measurement, a shape factor was calculated

$$C' = \frac{(F - F_0)\, T}{\sum_{i=1}^{I} n_i\, d_i^3} \qquad (29)$$

* Products, 200 EE and Eyemo, of Bell & Howell Co.

† Fluid, high-alumina cracking catalyst donated by W. R. Grace & Co.

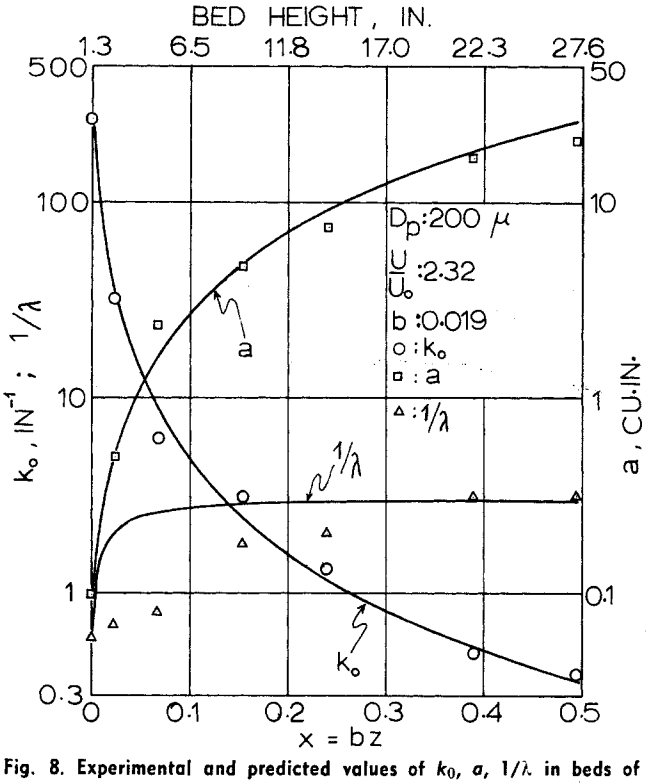

Fig. 8. Experimental and predicted values of k_0, a, $1/\lambda$ in beds of glass beads.

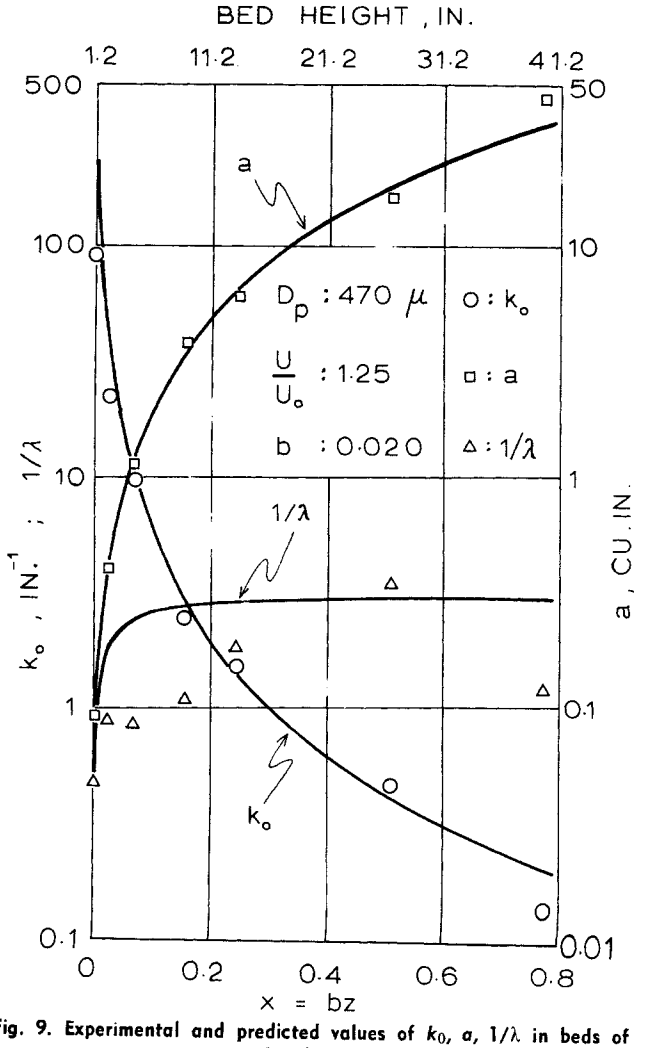

Fig. 9. Experimental and predicted values of k_0, a, $1/\lambda$ in beds of glass beads.

TABLE 3. SHAPE FACTORS OF BUBBLES BREAKING THE SURFACE

Material	Glass beads			Sand	Cracking catalyst
Average particle size, μ	470	200	85	160*	59
Average shape factor	0.240	0.153	0.0847	0.141*	0.125
Number of shape factors averaged	14	13	25	—	4
Standard deviation of shape factors	0.082	0.017	0.0299	—	0.0128

* Values calculated from the data of Harrison and Leung (*13*).

Shape factors at all bed heights and flow rates used, for the same material, were averaged. This average factor (Table 3) was used in calculating bubble volumes.

$$m_i = Cd_i^3 \tag{30}$$

The implicit assumption is that bubbles breaking the top surface of the fluidized bed are geometrically similar for a given material. This was verified by Harrison and Leung (*14*) in experiments with bubbles injected into a bed at incipient fluidization. They found relation (30) to hold for bubble diameters up to 75% the diameter of the column.

Bubble velocity was calculated by

$$v_i = A\, m_i^{1/6} \text{ in./sec.} \tag{31}$$

where A is a proportionality constant. Proposed by Davidson et al. (*15*), this relation was verified by these authors as well as by Harrison and Leung (*14*) and Rowe and Partridge (*16*) in experiments with injected bubbles and by Romero and Smith (*12*) in naturally bubbling beds. In each of these studies the value of the calculated constant was somewhat different. Rowe and Partridge found the constant to depend on particle size and shape, and their values are used here. Thus, the total variation in the value of the constant for the particles used becomes about 10%, and the average value

$$A = 14 \text{ in.}^{1/2}\text{/sec.} \tag{32}$$

is used throughout.

Next k_0, a, and $1/\lambda$ were calculated and compared to the values predicted by the model.

$$k_0 = \sum_{i=1}^{I} N_i \tag{33}$$

$$a = \frac{\sum_{i=1}^{I} N_i\, m_i}{\sum_{i=1}^{I} N_i} \tag{34}$$

$$1/\lambda = \frac{\sum_{i=1}^{I} N_i\, m_i^2}{k_0 a^2} - 1 \tag{35}$$

where

$$N_i = \frac{n_i}{v_i\, T} \tag{36}$$

is the number of bubbles of the i^{th} size per unit bed height.

Shape factors and values of k_0, a, and $1/\lambda$ obtained from the experimental data with the aid of Equations (29) to (36) are on file.*

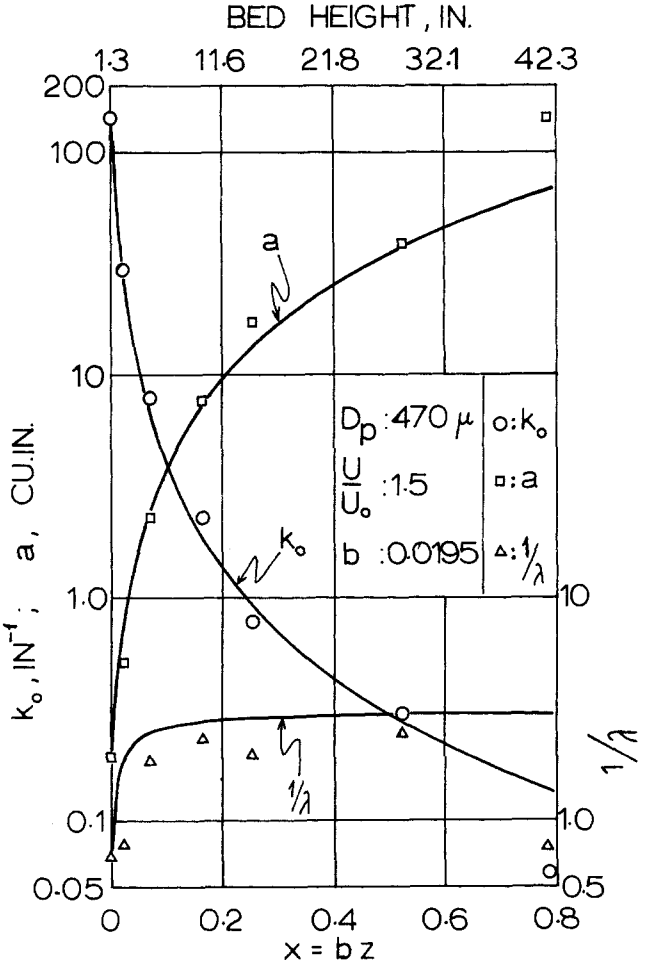

Fig. 10. Experimental and predicted values of k_0, a, $1/\lambda$ in beds of glass beads.

Error Analysis

The experimental distributions (*21*) resulted from two primary measurements: the projected diameter of a bubble (i.e., a length) and the number of bubbles. Although the magnitude of the error in measuring a length is known, there is no way to estimate the error in measuring the number of bubbles, especially in beds with a large number of small bubbles where a bubble could be missed or counted twice.

The effect of errors in measuring the projected diameter is shown in Figures 1 and 2. The dashed lines represent an upper and a lower limit for the cumulative distribution function $G(m)/k_0$ resulting from over- and underestimating all the projected diameters by an amount equal to the absolute maximum error.

* Tabular material has been deposited as document 01249 with the ASIS National Auxiliary Publications Service, c/o CCM Information Sciences, Inc., 22 W. 34th St., New York 10001 and may be obtained for $2.00 for microfiche or $5.00 for photocopies.

RESULTS

Photographs of bubbles breaking, or just about to break, the top bed surface at three different bed heights are shown in Figures 4, 5, and 6. In the three cases, glass beads of a 470μ average size were fluidized with air at 0.638 ft./sec. superficial velocity.

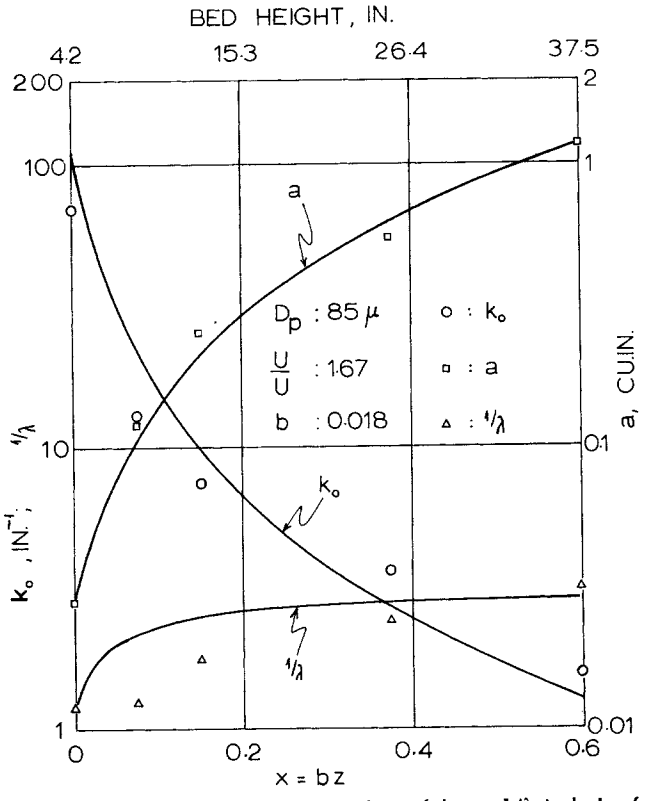

Fig. 11. Experimental and predicted values of k_0, a, $1/\lambda$ in beds of glass beads.

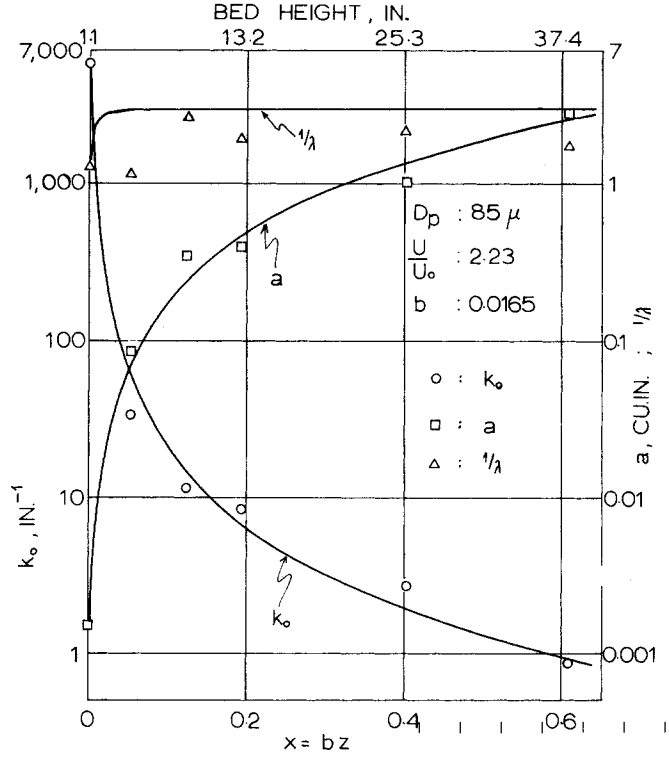

Fig. 12. Experimental and predicted values of k_0, a, $1/\lambda$ in beds of glass beads.

Table 4. Values of the Parameter of the Model

Material	D_p microns	U_0 ft./sec	U/U_0	b in.$^{-3/2}$
Glass beads	470	0.510	1.25	0.0200
			1.50	0.0195
	200	0.149	1.40	0.0150
			2.32	0.0190
	85	0.0263	1.67	0.0180
			2.23	0.0165
			3.34	0.0140
			4.46	0.0175*
			5.57	0.0175*
Cracking catalyst	59	0.0035	2.06	0.0260

* Arbitrary value.

Plots of k_0, a, and $1/\lambda$ vs. x predicted by the model are shown as solid lines in Figures 7 to 16. The experimental values of the variables are presented with the parameter b, obtained by a least-square fit of k_0 and a in each plot.

In Figures 9, 10, and 13 the points at the highest bed were not included in the least-squares fit. The bubbles were large compared to the column diameter, and the model was not expected to predict the observed values. The initial values of k_0, used to derive the profiles in Figures 6 and 8, are larger than the experimental values. This is because the bubble flow rate calculated from the motion pictures (using a shape factor averaged for the runs included in the plot) was lower than that calculated from flowmeter measurements. In both cases the initial value for k_0 was adjusted to correspond to the bubble flow rate obtained from flowmeter measurements. The experimental points in Figures 14 and 15 were too scattered and no fit was attempted. The theoretical lines were arbitrarily drawn to show the predicted trends.

In Figures 7 to 16 the effect of bed height on bubble population and volume is clearly seen. The total number of bubbles per unit bed height decreases very rapidly with increasing bed height while the mean bubble volume

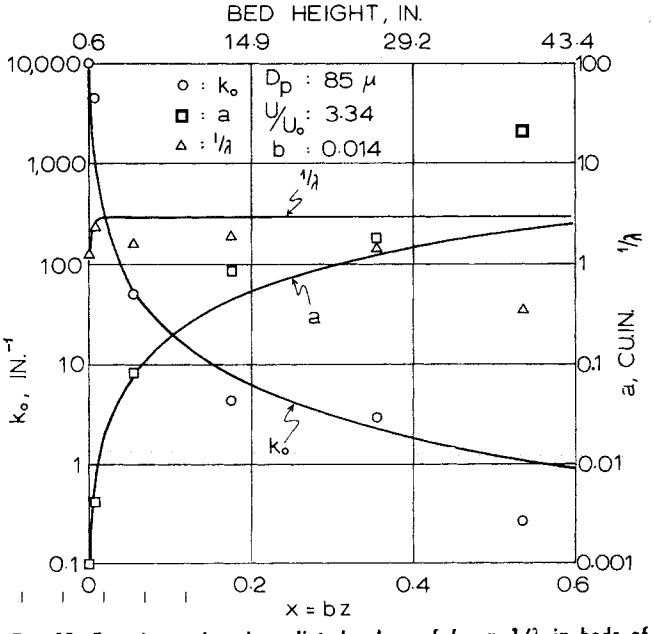

Fig. 13. Experimental and predicted values of k_0, a, $1/\lambda$ in beds of glass beads.

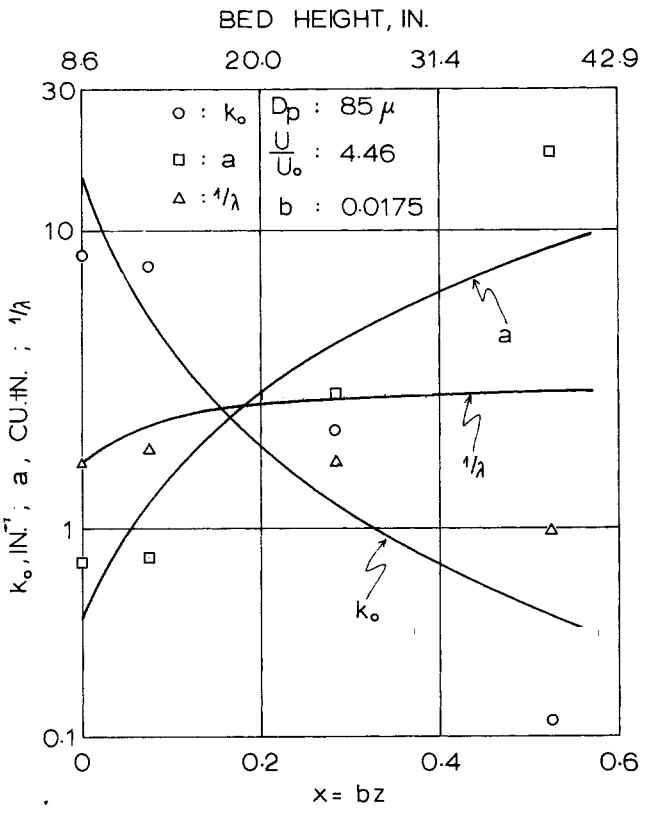

Fig. 14. Experimental and predicted values of k_0, a, $1/\lambda$ in beds of glass beads.

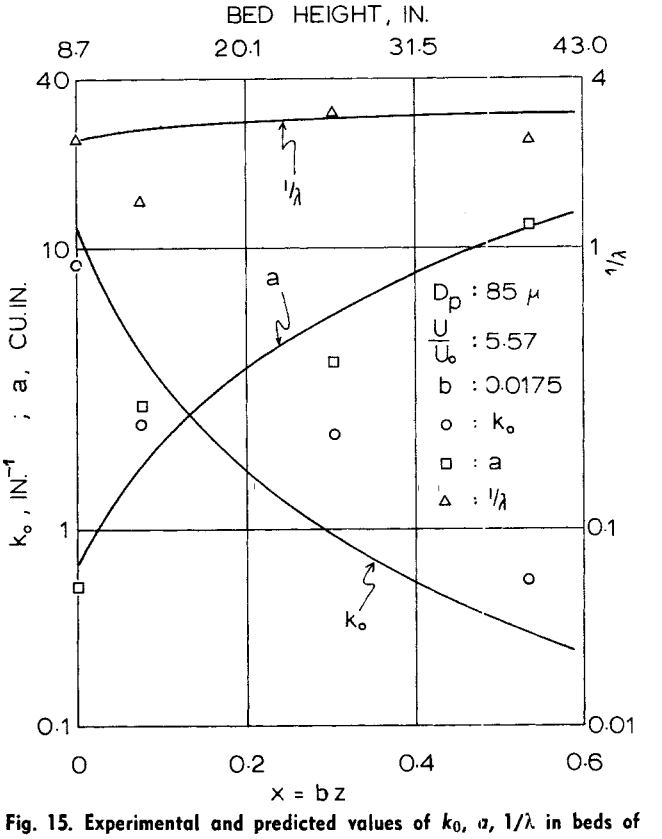

Fig. 15. Experimental and predicted values of k_0, a, $1/\lambda$ in beds of glass beads.

increases equally fast. The variance of the distribution, measured in units of squared mean, increases with bed height until it reaches a limiting value. The effect of velocity on k_0 and a is similar to that of bed height. At high velocities there are fewer larger bubbles per unit bed height. Velocity has no apparent effect on the variance.

Agreement between experimental and predicted values of k_0 and a is good. The model predicts higher values of $1/\lambda$ at lower bed heights and a limiting value $1/\lambda = 3.1$ at higher beds. This limiting value agrees with the experimentally obtained value of $1/\lambda$ for higher beds. The model does not predict the experimental values at higher beds at higher flow rates. This corresponds to larger bubble sizes where perhaps wall effects become important.

Values of the parameter b for each type of material and flow rate are listed in Table 4. Surprisingly, no trend was observed in the variation of the values of b with flow rate or particle size. We can also reevaluate B, which has an approximate magnitude of 27 in./sec. This velocity is of the same order of magnitudes as the velocity of the individual bubbles, which indicates that the main contribution to B might be the difference in velocity of bubbles of different size and that the collision efficiency must also be quite high.

More data in larger and higher beds are needed before one can conclude that this value of B applies also to industrial size fluidized beds. In the absence of other data, one might use the above value to get an approximate estimate of bubble size distribution in large beds. Of special interest is that, regardless of particle size and velocity, the bubbles continue to grow with height. Experiments in much larger and higher beds are needed to show whether bubbles do reach a limiting size, as sometimes postulated. If so, a considerable height is obviously required. In calculating the mass transfer from the bubbles to the fluidized bed, this requirement as well as the

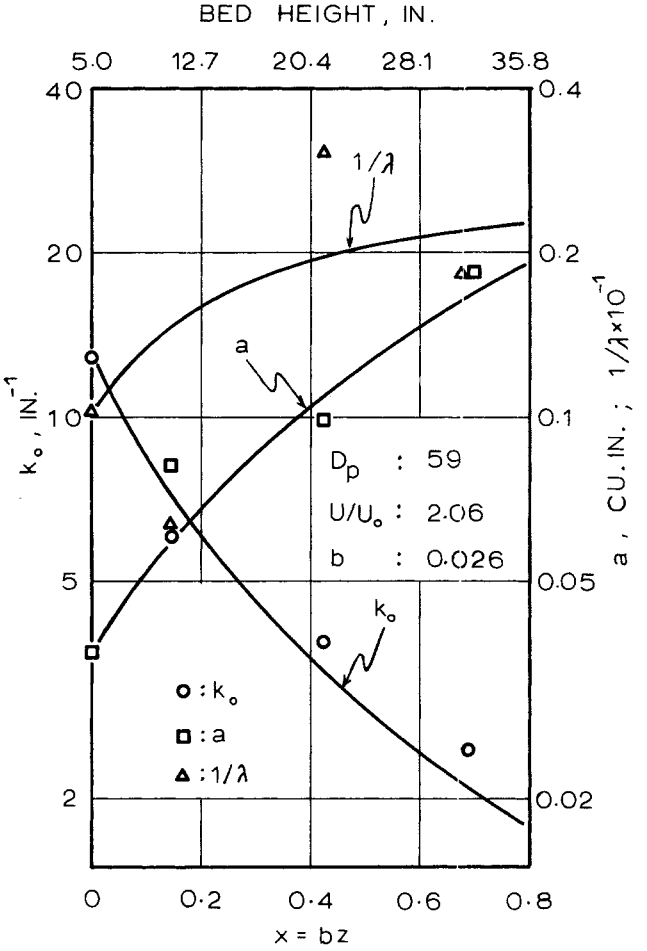

Fig. 16. Experimental and predicted values of k_0, a, $1/\lambda$ in beds of cracking catalyst.

wide size distribution of the bubbles should be taken into account.

CONCLUSIONS

The determination of bubble volumes by taking motion pictures of the top surface of the bed and measuring the diameter of the bubbles breaking surface is a convenient way to study bubble growth in gas fluidized beds. However, determination of a shape factor for the material used, which relates the diameter of the bubble breaking surface to the bubble volume, is necessary.

A model of bubble growth by coalescence in gas fluidized beds was established. The proportionality constant of the proposed mechanism may be considered as a representation of the velocity differences of the colliding bubbles. In this study it was assumed to be independent of bubble volume and was obtained from the experimental results. The model predicted the change in average bubble size and in the number of bubbles per unit bed height for small and moderate bubble sizes. The collision parameter of the model appears to be independent of gas flow rate and particle size. When the bubble diameters approach that of the column, the model does not predict the observed distributions.

A striking feature of a bubbling gas-fluidized bed was the fast rate of bubble growth. The number of bubbles per unit bed height was found to decrease by three or more orders of magnitude over three feet of bed height while the average bubble volume increased by an equivalent amount. The results did not show when an equilibrium maximum bubble size is reached.

Growth by coalescence, therefore, is an important process in the "life" of a bubble as it moves up the bed. This process should be taken into account in setting up models of bubbling gas-fluidized beds for mass or heat transfer or chemical reaction between gas and fluidized particles, instead of considering the bubbles all of the same size and uniformly distributed throughout the bed.

ACKNOWLEDGMENT

The authors wish to thank Dr. Stanley Katz of the City University of New York for his valuable suggestions on the mathematical treatment. This work is part of the research carried out by Dr. D. T. Argyriou at the City University of New York in partial fulfilment of the requirements of the Ph. D. degree.

NOTATION

a = mean bubble volume, cu. in.
A = constant in the velocity expression (6) in.$^{1/2}$/sec.
B = proportionality constant in the collision mechanism, in. sec.$^{-1}$
b = parameter of the model, in.$^{-3/2}$
C' = shape factor relating bubble volume to the diameter of the bubble breaking surface
C = shape factor averaged for the material
d = diameter of bubble breaking the top surface of the bed, in.
d_i = diameter of bubbles of i^{th} size breaking top surface of bed, in.
D_p = average particle diameter, μ
f = number density of bubbles, in.$^{-4}$
F = gas flow rate, cu.in./sec.
F_o = gas flow rate at incipient fluidization, cu.in./sec.
G = incomplete gamma function
h = source function, in.$^{-4}$ sec.$^{-1}$
H = bed height, in.
H_0 = settled bed height, in.
I = total number of different bubble sizes in a run
k_0 = number of bubbles per unit bed height, in.$^{-1}$
L = associate Laguerre polynomials
m = bubble volume, cu.in.
n_i = number of bubbles of diameter d_i
N_i = number of bubbles of diameter d_i per unit bed height, in.$^{-1}$
p = gamma distribution
r_f = rate of bubble formation by coalescence, in.$^{-4}$ sec.$^{-1}$
r_e = rate of disappearance of bubbles because of collision, in.$^{-4}$ sec.$^{-1}$
S = cross sectional area of bed, sq.in.
t = time coordinate, sec.
T = time interval of a run, sec.
U = superficial air velocity, ft./sec.
U_0 = superficial air velocity at incipient fluidization, ft./sec.
v = bubble velocity, in./sec.
x = transformed space coordinate ($= bz$), in.$^{-5/2}$
z = space coordinate, in.

Greek Letters

Γ = gamma function
λ = dependent variable, related to the variance of bubble volumes, defined by Equation (18)
μ_j = J^{th} moment of m. Defined by Equation (8)
ψ = digamma function

LITERATURE CITED

1. Hulburt, H. M., and Stanley Katz, *Chem. Eng. Sci.*, **19**, 555 (1964).
2. Partridge, B. A., and P. N. Rowe, *Trans. Inst. Chem. Engrs. (London)*, **44**, T335 (1966).
3. *Ibid.*, T349.
4. Ohmae, Tsutomu, and Junji Furukawa, *J. Chem. Soc. Japan, Ind. Chem. Sect.*, **56**, 909 (1953).
5. Mathis, J. F., and C. C. Watson, *AIChE J.*, **2**, 578 (1956).
6. Morse, R. D., and C. O. Ballou, *Chem. Eng. Progr.*, **47**, 199 (1951).
7. Yasui, George, and L. N. Johanson, *AIChE J.*, **4**, 445 (1958).
8. Lanneau, K. P., *Trans. Inst. Chem. Engrs. (London)*, **38**, 125 (1960).
9. Porter, James D., Ph.D. thesis, Mass. Inst. Technol., Cambridge (1963).
10. Grohse, E. W., *AIChE J.*, **1**, 358 (1955).
11. Baumgarten, P. K., and R. L. Pigford, *ibid.*, **6**, 115 (1960).
12. Romero, J. B., and D. W. Smith, *ibid.*, **11**, 595 (1965).
13. Harrison, D., and L. S. Leung, "Symposium on the Interacting between Fluids and Particles," p. 127, Inst. Chem. Engrs., London (1962).
14. ———, *Trans. Inst. Chem. Engrs. (London)*, **40**, 146 (1962).
15. Davidson, J. F., R. C. Paul, M. J. S. Smith, and M. A. Duxbury, *ibid.*, **73**, 232 (1959).
16. Rowe, P. N., and B. A. Partridge, *ibid.*, **43**, 157 (1965).
17. Abramowitz, Milton, and I. A. Stegun, ed., "Handbook of Mathematical Functions," p. 253, Natl. Bur. Std., Washington, D.C. (1964).
18. Jackson, R., *Trans. Inst. Chem. Engrs., (London)*, **41**, 13 (1963).
19. Pigford, R. L., and T. Baron, *Ind. Eng. Chem. Fundamentals*, **4**, 81 (1965).
20. Davidson, J. F., and Harrison, D., "Fluidised Particles," p. 85, Cambridge Univ. Press, London (1963).
21. Argyriou, D. T., Ph.D. thesis, The City University of New York (1968); microfilmed by University Microfilms Inc., Ann Arbor, Michigan.

Manuscript received August 31, 1967; revision received May 8, 1969; paper accepted May 9, 1969. Paper presented at AIChE New York meeting.